

Short communication

# Fabrication and testing of coplanar single-chamber micro solid oxide fuel cells with geometrically complex electrodes

Melanie Kuhn<sup>a</sup>, Teko Napporn<sup>b</sup>, Michel Meunier<sup>b</sup>, Daniel Therriault<sup>a</sup>, Srikar Vengallatore<sup>c,\*</sup>

<sup>a</sup> Department of Mechanical Engineering, École Polytechnique de Montréal, 2900 Boulevard Edouard-Montpetit, Montreal, H3T 1J4 Canada

<sup>b</sup> Department of Engineering Physics, École Polytechnique de Montréal, 2900 Boulevard Edouard-Montpetit, Montreal, H3T 1J4 Canada

<sup>c</sup> Department of Mechanical Engineering, McGill University, 817 Sherbrooke Street West, Room 363, Montreal, Quebec, H3A 2K6 Canada

Received 27 August 2007; received in revised form 26 October 2007; accepted 5 November 2007

Available online 17 November 2007

## Abstract

Coplanar single-chamber micro solid oxide fuel cells (SC- $\mu$ SOFCs) with curvilinear microelectrode configurations of arbitrarily complex two-dimensional geometry were fabricated by a direct-write microfabrication technique using conventional fuel cell materials. The electrochemical performance of two SC- $\mu$ SOFCs with different electrode shapes, but comparable electrode and inter-electrode dimensions, was characterized in a methane–air mixture at 700 °C. Both cells exhibited stable open circuit voltage and peak power density of 0.9 V and 2.3 mW cm<sup>-2</sup>, respectively, indicating that electrode shape did not have a significant influence on the performance of these fuel cells.

© 2007 Elsevier B.V. All rights reserved.

**Keywords:** Single-chamber solid oxide fuel cell; SOFC; Microfabrication; Direct-writing; Portable power generation; MEMS

## 1. Introduction

The increasing demand for miniaturized power generators with high energy density, reliable operation, and fast regeneration is motivated by the rapid proliferation of consumer electronics and the steady commercialization of a wide variety of microelectromechanical systems (MEMS). The development of efficient energy systems beyond conventional battery technology is required to meet this demand [1]. Miniaturized solid oxide fuel cells (SOFCs) are one of the many concepts currently under development for portable power generation in such small-scale portable applications. SOFCs are attractive because the elevated operating temperatures (300–750 °C) enable the efficient use of hydrocarbon fuels with high energy densities [2].

Single-chamber solid oxide fuel cells (SC-SOFCs) are well suited for miniaturization and integration with MEMS [3]. Conventional dual-chamber fuel cells require high-temperature gas-tight sealing to keep the fuel (hydrocarbon) and oxidant (air) isolated at all times. In contrast, SC-SOFCs operate on

mixtures of fuel and air [4–6], thereby removing the necessity of high-temperature sealing and complex gas manifolding. SC-SOFCs can be operated in several designs including a coplanar single-face configuration in which both electrodes, i.e., anode and cathode, are situated on the same side of a planar electrolyte [7–13]. This configuration enables the use of thick electrolytes for better thermomechanical stability and reliability during high-temperature operation. Furthermore, multiple SC-SOFCs can easily be connected in parallel and/or series to meet the power demand of portable devices [7].

Coplanar single-chamber SOFCs in the single-face configuration are a relatively recent development and correlations between processing, structure, properties, performance, and reliability are only now emerging. The studies reported in the literature have focused on fuel cells in which the anodes and cathodes are either a pair of parallel straight lines [7,8,13], or interdigitated structures with multiple pairs of parallel lines [9–13]. In addition to the effects of reactant gas composition and gas flow direction [8,10], it has been established that the inter-electrode width has a significant effect on power generation. The ohmic resistance for ionic conduction through the electrolyte is determined by the distance between adjacent electrodes and, hence, reducing inter-electrode spacings has been demonstrated to improve fuel cell performance [7,8,10,14,15].

\* Corresponding author. Tel.: +1 514 398 2174; fax: +1 514 398 7365.  
E-mail address: [srikar.vengallatore@mcgill.ca](mailto:srikar.vengallatore@mcgill.ca) (S. Vengallatore).

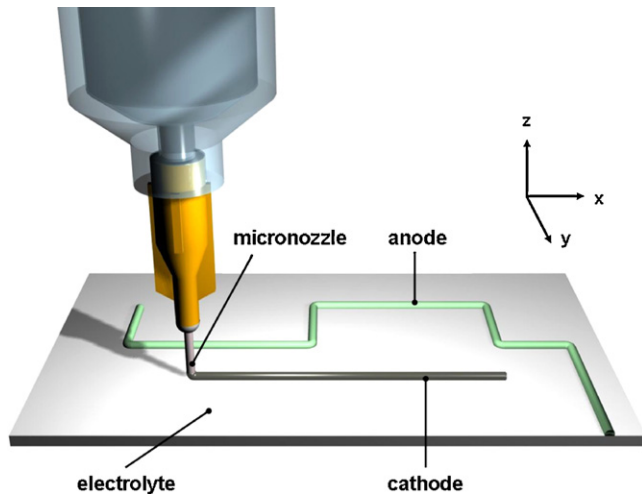


Fig. 1. Schematic illustration of direct-write microfabrication. The direct-write technique consists of the pressure-driven extrusion of a paste-like material or suspension through fine micronozzles. The desired pattern is generated by the robot-controlled deposition of the extruded continuous filaments on a substrate.

Robot-controlled direct-write microfabrication techniques are emerging as a simple and convenient method for fabricating SC- $\mu$ SOFCs in the single-face configuration [10,11]. Direct-writing allows the rapid fabrication of complex microscale structures and geometries using a wide variety of materials without the need for expensive photomasks [16]. The essential concepts in this approach are to prepare suspensions (or inks) using powders of electrode materials, and then to extrude the suspensions through a micronozzle onto the electrolyte substrate in the desired pattern, as illustrated in Fig. 1.

The single-face configuration is compatible with the design of closely spaced electrodes in a variety of geometries. However, many critical issues associated with the use of complex curvilinear shapes for electrodes in SC- $\mu$ SOFCs remain unexplored. These include the manufacturing limitations of microfabricating geometrically complex electrodes and the effects of electrode shape on fuel cell performance. The latter has implications for fuel cell modelling and optimized structural design. For these reasons, it is important to understand the relationships between microfabrication processes, electrode shape and structure, and the power and voltage generated by the fuel cell. As a first step towards that goal, this paper presents experimental results on direct-write microfabrication and electrochemical testing of coplanar SC- $\mu$ SOFCs with electrodes of curvilinear two-dimensional geometry.

## 2. Experimental details

Conventional SOFC materials were used for anode, cathode, and electrolyte in this study. For the anode, NiO powder (lot number: GRD-5, median particle size:  $0.56\ \mu\text{m}$ , density:  $6.7\ \text{g cm}^{-3}$ , surface area:  $6.3\ \text{m}^2\ \text{g}^{-1}$ ) was mixed with an YSZ powder (zirconia stabilized with 8 mol% yttria, lot number: 1606, median particle size:  $0.25\ \mu\text{m}$ , density:  $5.99\ \text{g cm}^{-3}$ , surface area:  $6.1\ \text{m}^2\ \text{g}^{-1}$ ) in a ratio of 55 wt% NiO and 45 wt% YSZ. The powder mixture was thoroughly ball-milled

using a Spex Mixer/Mill for 12 h. The cathode material was  $(\text{La}_{0.8}\text{Sr}_{0.2})_{0.98}\text{MnO}_3$  (LSM) powder with a median particle size of  $0.63\ \mu\text{m}$ , density of  $6.4\ \text{g cm}^{-3}$ , and surface area of  $4.24\ \text{m}^2\ \text{g}^{-1}$  (lot number: 155-66). All powders were purchased from NexTech Materials. 0.2 mm thick YSZ plates (Marketech) were used as the electrolyte.

The electrode suspensions must be prepared so as to permit uniform flow of the suspensions through the micronozzle during deposition, and to ensure that the deposited structure retains its shape after extrusion. In turn, these characteristics are governed by the particle loading and the rheological properties of the suspension. Based on guidelines developed in a previous study [11], electrode suspensions with a particle loading of 16 vol% (equivalent to 56 wt%) were prepared by colloidal processing of the anode and cathode powders. A mixture of powder, solvent (Terpineol, J.T. Baker), dispersant (Triton X-100, Alfa Aesar) and binder (poly(vinyl butyral-co-vinyl-alcohol-co-vinyl acetate), Sigma-Aldrich) was ball-milled in the Spex Mixer/Mill for 1 h. The electrode suspensions were poured in a syringe barrel ( $3\ \text{cm}^3$ , EFD Inc.) and then extruded under constant pressure through high precision stainless steel micronozzles (EFD Inc., inner nozzle diameter:  $150\ \mu\text{m}$ ).

The direct-write technique used for the fabrication of the SC- $\mu$ SOFCs in the single-face configuration has been described extensively, along with process-structure correlations, in a recent publication [11]. The essential details are as follows. A robotic deposition apparatus (I & J 2200-4, I & J Fisnar Inc.) was used for direct-write microfabrication of the desired electrode geometry on the YSZ plate. With respect to the coordinates shown in Fig. 1, the electrolyte substrate was mounted on a mobile, robot-controlled stage that could move in the  $x$ -direction, whereas the micronozzle was able to move in  $y$ - and  $z$ -direction. The distance between the nozzle and substrate was on the order of the nozzle diameter. An extrusion pressure of  $\sim 870\ \text{kPa}$  for the anode and  $\sim 700\ \text{kPa}$  for the cathode was applied while the robot velocity was fixed at  $0.3\ \text{mm s}^{-1}$  for a total electrode deposition time of less than 4 min. The anode structure was deposited first and sintered at  $1250\ ^\circ\text{C}$  for 3 h under ambient atmosphere. Subsequently, the cathode was deposited and the structure was sintered at  $1100\ ^\circ\text{C}$  for 3 h to complete the fabrication of the SC- $\mu$ SOFC.

Preliminary depositions were performed to confirm that electrodes of different designs (including wave-like, triangular, and spiral geometries) could be obtained using direct-writing. Subsequently, two different illustrative designs of SC- $\mu$ SOFCs were fabricated using the same feedstock materials for electrodes and electrolyte. The electrodes of these fuel cells contained a combination of curvilinear electrodes to spell “SOFC” and “POLY”, respectively (Fig. 2). The electrode dimensions and average inter-electrode spacings were designed to be constant, so that a comparison of the performance of these devices can isolate the effects of electrode shape from size.

The electrode dimensions and inter-electrode distances were measured from optical micrographs obtained using an Olympus SZX12 stereomicroscope and by using image-processing software (Image-Pro Plus 6.2). Twenty measurements were performed to determine each electrode width and inter-electrode

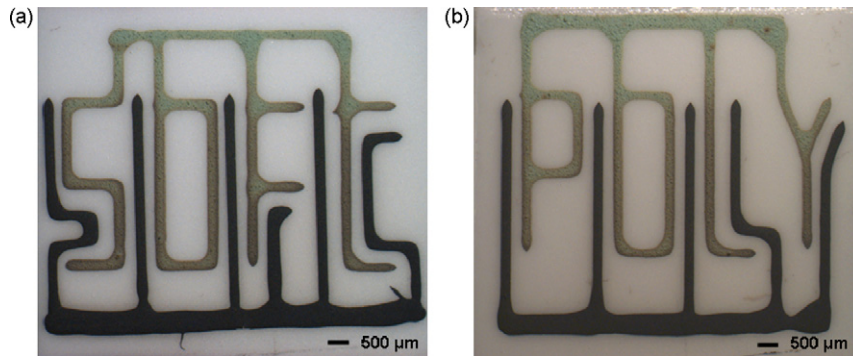


Fig. 2. Optical micrographs of single-chamber micro solid oxide fuel cells in single-face configuration with curvilinear electrode geometries. These images were taken after sintering (and before electrochemical testing).

distance. The anodes constitute the letters of the words “SOFC” and “POLY”, and the cathodes are the adjacent straight line segments. The inter-electrode distance is a measure of the spacing between adjacent electrodes and was measured perpendicular to the orientation of the cathode segments. This choice enables a close comparison with SC- $\mu$ SOFCs with interdigitated comb-like electrodes [11]. The electrode surface areas listed in Table 1 includes the connecting lines on which the gold current collectors were placed during electrochemical testing. The measurement resolution (i.e., pixel size) was  $\sim 8 \mu\text{m}$  at the magnification used. A scanning electron microscope (SEM, Quanta FEG 200, FEI Instruments) was used to investigate the microstructure of the electrodes after sintering. The grain size and the electrode porosity were evaluated through SEM image analysis.

The electrochemical performance of the fabricated SC- $\mu$ SOFCs was tested using a high-temperature testing setup that has been described previously [6,17]. The fuel cells were operated in methane–air mixtures that are characterized by the methane-to-oxygen ratio,  $R_{\text{mix}}$ . A methane–air mixture with a total flow rate of 150 sccm and a ratio  $R_{\text{mix}} = 2$  was used in testing. Additional nitrogen (with a flow rate of about 700 sccm) was used as a shielding gas to facilitate gas transport over the fuel cells. The furnace temperature was set to 700 °C. Gold wire and grid (Alfa Aesar) served as current collectors. A gold grid was placed over the connecting lines (that is, the horizontal elec-

trode segments that connect all the anodes and all the cathodes on each fuel cell). Subsequently, a gold wire was attached to the grids to facilitate electrical measurements. The NiO anode was reduced to nickel in a methane/nitrogen mixture before introducing oxygen into the furnace. The temperature of 700 °C indicated throughout this paper refers to the preset furnace temperature. The actual cell temperature was measured to be between 720 and 740 °C using the procedure described by Napporn et al. [6].

### 3. Results and discussion

The two electrode geometries are shown in Fig. 2a and b. In these micrographs, anode and cathode appear in green and black, respectively. Thus, the anodes spell the letters “SOFC” and “POLY”, while the cathode is composed of closely spaced linear segments between the letters. Table 1 summarizes the minimum, mean, maximum, and standard deviation ( $\sigma$ ) of the electrode width for each fuel cell. Also listed are the dimensions of the inter-electrode area in terms of the average inter-electrode distance and the length of the overlapping electrode segments. The variations in electrode widths (5% variation in mean values, and standard deviations that are  $\sim 10\%$  of mean values) are an indication of the manufacturing tolerance associated with direct-write microfabrication. Details on the source of these variations are discussed in a recent paper [11] which investigated the relationships between process parameters (especially, ink viscosity,

Table 1  
Electrode dimensions and inter-electrode spacings of the SC- $\mu$ SOFCs

		“SOFC” geometry		“POLY” geometry	
		Anode	Cathode	Anode	Cathode
Electrode surface area ( $\text{cm}^2$ )	Mean	0.129	0.115	0.107	0.111
Electrode width ( $\mu\text{m}$ )	Minimum	200	202	176	221
	Mean	251	263	229	242
	Maximum	283	400	265	346
	$\sigma$	19	36	15	14
Inter-electrode distance ( $\mu\text{m}$ )	Minimum		158		176
	Mean		434		487
	Maximum		1525		1557
	$\sigma$		392		448
Length of overlapping electrode segments (mm)	Mean		4.4		4.0

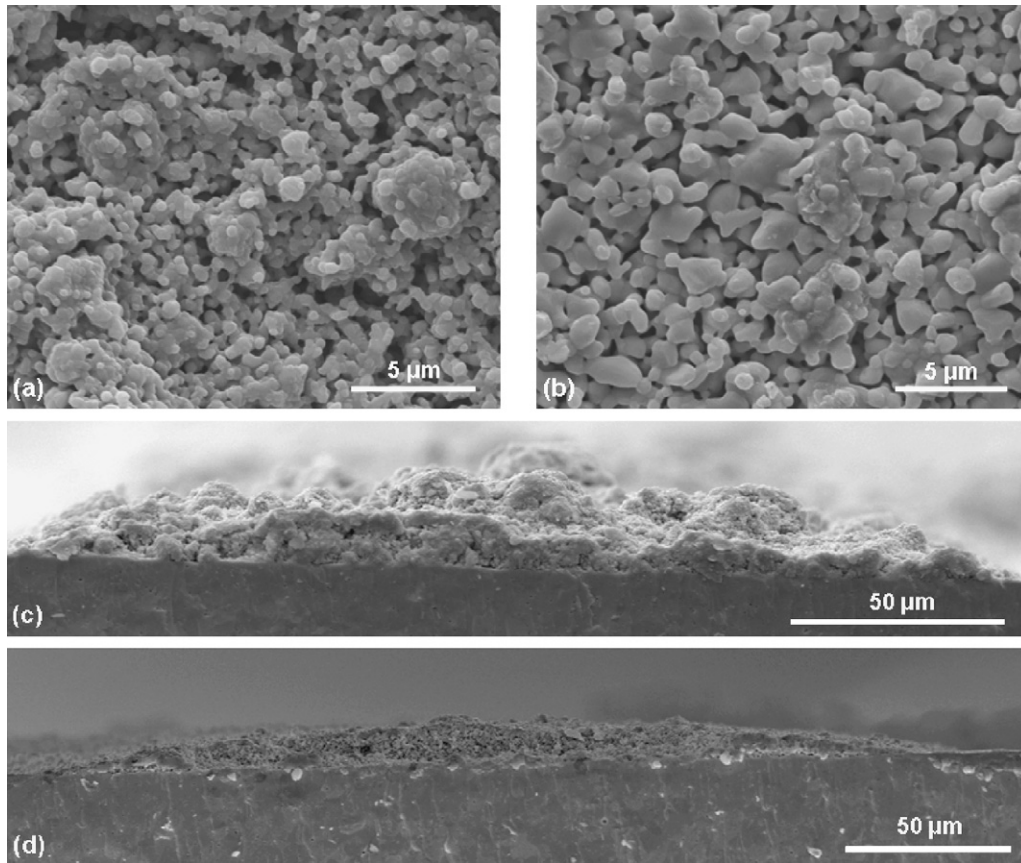


Fig. 3. Scanning electron micrographs of the sintered electrodes showing plan views of anode (a) and cathode (b), and cross-sectional views of anode (c) and cathode (d).

extrusion pressure, and stage velocity) and the dimensions and continuity of deposited electrodes.

Fig. 3 shows representative scanning electron microscope images of the microstructure of the sintered anode and cathode. The anode exhibited an average grain size of less than  $1\ \mu\text{m}$  (Fig. 4a). The porosity was heterogeneous due to the presence of small pores with an average size of less than  $1\ \mu\text{m}$  and the presence of several larger pores. In comparison, the microstructure of the cathode was more homogeneous with pore sizes ranging from  $0.5$  to  $2\ \mu\text{m}$  (Fig. 3b). The cross-sectional shape of a typ-

ical anode and cathode is shown in Fig. 3c and d, respectively. The sidewalls of the electrodes formed a lens-like shape due to the spreading of the electrode suspension on the YSZ substrate during direct-write microfabrication. The maximum electrode thickness ranged between  $12$  and  $20\ \mu\text{m}$ . Notably, no differences were found between the microstructures of the electrodes in the two different fuel cells.

Electrochemical testing of the SC- $\mu$ SOFCs was performed at  $700\ ^\circ\text{C}$  in a methane–air mixture ( $R_{\text{mix}} = 2$ ) and at a total gas flow of  $150\ \text{sccm}$ . The gas flow direction was from left to right with

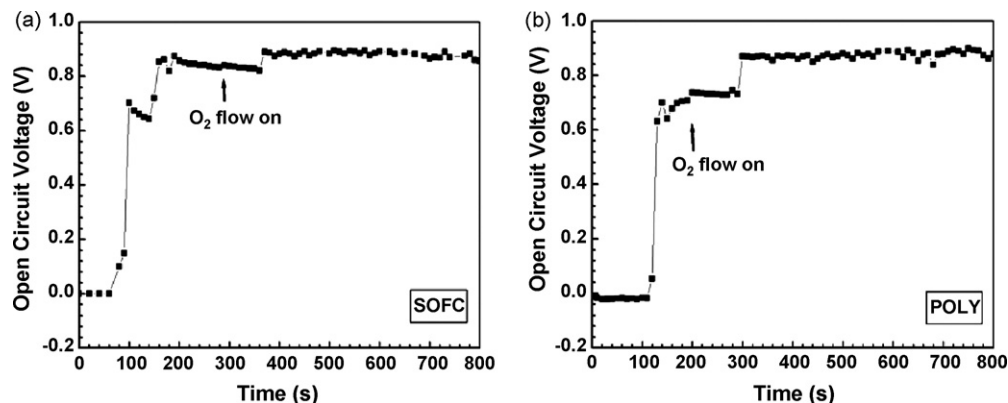


Fig. 4. Open circuit voltage as a function of time for (a) “SOFC” and (b) “POLY” electrode geometry during fuel cell operation in a methane–air mixture (methane-to-oxygen ratio  $R_{\text{mix}} = 2$ ) at  $700\ ^\circ\text{C}$  and a gas flow rate of  $150\ \text{sccm}$ . The methane/nitrogen mixture was allowed to flow over the cell at  $t = 0\ \text{s}$ .

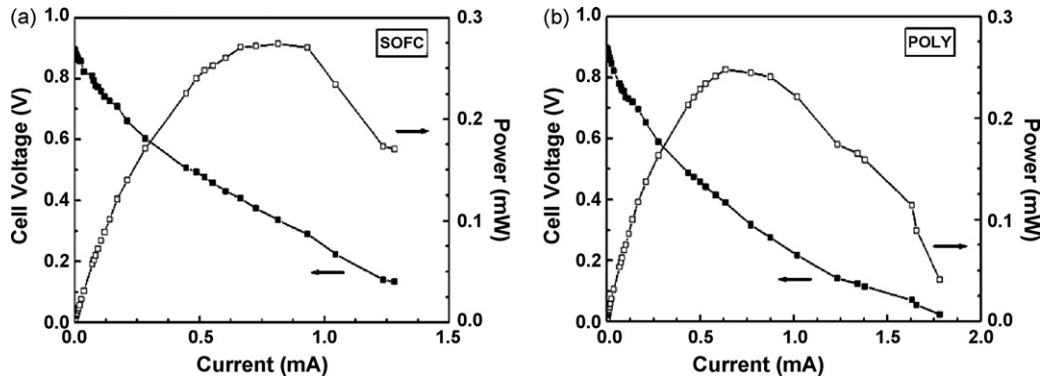


Fig. 5. Voltage current characteristics of the (a) “SOFC” and (b) “POLY” geometry. Both tests were performed in a methane–air mixture with  $R_{\text{mix}} = 2$  and a total gas flow of 150 sccm at 700 °C.

respect to the micrographs in Fig. 2a and b. The time responses of the open circuit voltage (OCV) following exposure to the gas mixture are shown in Fig. 4a and b. At time  $t=0$  s, the methane/nitrogen mixture is introduced into the chamber and this leads to the establishment of a transient open circuit voltage of  $\sim 0.6$  V before oxygen is introduced into the chamber. Now, once oxygen is added to the gas mixture, the OCV increases further to  $\sim 0.9$  V, and remains stable at this value for both fuel cells. There are no significant differences in the response of the two fuel cells, and it is concluded that electrode shape does not affect the open-circuit voltage.

The recent experimental studies of Morel et al. [18] provide valuable insight into the mechanisms responsible for the time response of the OCV. In that study, the reduction processes of NiO anodes of SC-SOFCs were studied by analyzing the outlet gas compositions in real time using a quadrupole mass spectrometer. The dominant reaction under a  $\text{CH}_4$  flow at 700 °C was the reduction of NiO leading to the formation of CO and  $\text{H}_2$  gases, along with a smaller amount of  $\text{CO}_2$ . The presence of the syngas at the anode/electrolyte interface creates a transient open circuit voltage even without the addition of oxygen. In addition, the cracking of methane is accompanied by carbon deposition on the electrodes. The introduction of oxygen leads to decarburization followed by a further increase of the OCV to the stable value of 0.9 V.

Fig. 5 shows the voltage–current characteristics for the two SC- $\mu$ SOFCs at 700 °C in a methane–air mixture with  $R_{\text{mix}} = 2$ . The maximum power generated is 0.27 mW and 0.25 mW for the “SOFC” and “POLY” designs, respectively. However, since the electrode sizes are not identical in both cells, a normalized comparison is necessary to evaluate the effects of shape on performance.

The measured power can be scaled using either the average area of one electrode, or the total area of the fuel cell [13], as normalizing parameters. Here, the former choice is adopted since it can lead to a close comparison with the performance of conventional SOFCs. That is, the performance of trilayered dual-chamber fuel cells is typically normalized with respect to the electrode areas, since these represent the electron generating surfaces. The thickness of the electrolyte, which is a measure of the ionic resistance, is not typically considered in normalizing the performance of such fuel cells. Similarly, in SC- $\mu$ SOFCs

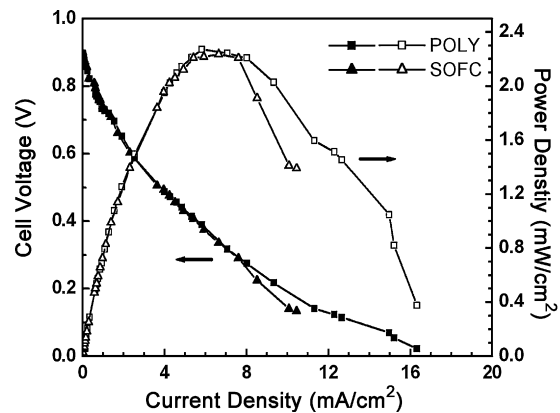


Fig. 6. Comparison of the electrochemical performance of the “SOFC” and “POLY” geometry in a methane–air mixture with  $R_{\text{mix}} = 2$  and a total gas flow of 150 sccm at 700 °C. Voltage (closed symbols) and power density (open symbols) are plotted as functions of current density. The average electrode surface area is the normalization parameter.

with interdigitated electrodes, the average electrode area represents the electron generating surfaces, and the inter-electrode area (which is a measure of ionic resistance) is ignored in normalization.

Fig. 6 shows the voltage and power density as functions of current density normalized with respect to the average electrode area. Both fuel cells exhibit a peak power density of  $2.3 \text{ mW cm}^{-2}$ , and this comparison suggests that in-plane electrode shape has no significant effect on electrochemical performance of these SC- $\mu$ SOFCs. Therefore, there is no significant benefit in designing SC- $\mu$ SOFCs with geometrically complex electrodes. However, additional testing of such fuel cells under different conditions (particularly the direction of gas flow with respect to electrode geometry) and using different fuel cell materials is necessary to confirm these preliminary results.

#### 4. Conclusions

This paper is the first report of direct-write microfabrication and electrochemical testing of single-chamber micro solid oxide fuel cells with geometrically complex electrodes. Two different SC- $\mu$ SOFC designs were tested under identical conditions of gas composition, flow direction, and furnace temperature.

Both fuel cells exhibited identical open circuit voltage and peak power density of 0.9 V and 2.3 mW cm<sup>-2</sup>, respectively, at 700 °C. These results demonstrate the versatility of the direct-write microfabrication method for manufacturing SC- $\mu$ SOFCS, and suggest that electrode shape does not have a significant impact on the performance of coplanar SC- $\mu$ SOFCS.

### Acknowledgements

The authors gratefully acknowledge funding for this project by the Fonds Québécois de la Recherche sur la Nature et les Technologies (FQRNT) and the Canadian Foundation for innovation. Financial support for M. Kuhn was provided by the government of Québec (doctoral research scholarship by FQRNT).

### References

- [1] C.K. Dyer, J. Power Sources 106 (2002) 31–34.
- [2] S. Park, J.M. Vohs, R.J. Gorte, Nature 404 (2000) 265–267.
- [3] G.J. La O', H.J. In, E. Crumlin, G. Barbastathis, Y. Shao-Horn, Int. J. Energy Res. 31 (2007) 548–575.
- [4] T. Hibino, H. Iwahara, Chem. Lett. 7 (1993) 1131–1134.
- [5] Z. Shao, S.M. Haile, J. Ahn, P.D. Ronney, Z. Zhan, S.A. Barnett, Nature 435 (2005) 795–798.
- [6] T. Napporn, F. Morin, M. Meunier, Electrochem. Solid State Lett. 7 (2004) A60–A62.
- [7] T. Hibino, K. Ushiki, Y. Kuwahara, Solid State Ionics 91 (1996) 69–74.
- [8] X. Jacques-Bedard, T.W. Napporn, R. Roberge, M. Meunier, J. Electrochem. Soc. 154 (2007) B305–B309.
- [9] S.-J. Ahn, J.-H. Lee, J. Kim, J. Moon, Electrochem. Solid State Lett. 9 (2006) A228–A231.
- [10] S.-J. Ahn, Y.-B. Kim, J. Moon, J.-H. Lee, J. Kim, J. Power Sources 171 (2007) 511–516.
- [11] M. Kuhn, T. Napporn, M. Meunier, S. Vengallatore, D. Therriault, J. Micromech. Microeng. 18 (2008) 015005.
- [12] S.P. Yoon, H.J. Kim, B.-T. Park, S.W. Nam, J. Han, T.-H. Lim, S.-A. Hong, J. Fuel Cell Sci. Technol. 3 (2006) 83–86.
- [13] B.E. Buegler, M. Ochsner, S. Vuillemin, L.J. Gauckler, J. Power Sources 171 (2007) 310–320.
- [14] J. Fleig, H.L. Tuller, J. Maier, Solid State Ionics 174 (2004) 261–270.
- [15] C.Y. Chung, Y.C. Chung, J. Kim, J. Lee, H.W. Lee, J. Electroceram. 17 (2006) 959–964.
- [16] J.A. Lewis, Curr. Opin. Solid State Mater. Sci. 6 (2002) 245–250.
- [17] T.W. Napporn, X. Jacques-Bedard, F. Morin, M. Meunier, J. Electrochem. Soc. 151 (2004) A2088–A2094.
- [18] B. Morel, S. Savoie, R. Roberge, T.W. Napporn, M. Meunier, in: U. Bossel (Ed.), Proceedings of the Seventh European SOFC Forum, CD-ROM, Lucerne, Switzerland, 2006, p. P1105.